

Microfluid Nanofluid (2012) 13:29–35
DOI 10.1007/s10404-012-0937-3

RESEARCH PAPER

Nano-slit electrospray emitters fabricated by a micro- to nanofluidic via technology

M. Dijkstra · J. W. Berenschot · M. J. de Boer ·
H. J. van der Linden · T. Hankemeier · T. S. J. Lammerink ·
R. J. Wiegink · M. Elwenspoek · N. R. Tas

Received: 20 September 2011 / Accepted: 21 November 2011 / Published online: 2 March 2012
© The Author(s) 2012. This article is published with open access at Springerlink.com

Abstract This article presents nano-slit electrospray emitters fabricated by a micro- to nanofluidic via technology. The main advantage of the technology is the ability to position freely suspended nanochannels anywhere on a microfluidic chip, where leak-tight delivery of fluid from a fluid reservoir can be established through long microchannels. The technology has proven to be useful in creating electrospray emitters coupled to freely suspended microchannels. It was observed that filling of nanochannels through via connections with integrated microchannels occurs not only due to bulk capillary action. These observations lead to a redesign of the electrospray chips. Repeatable electrospray IV-curves could be obtained from fabricated nano-slit electrospray emitters. Moreover, integration of on-chip microfluidic components is one of the possibilities of the fluidic via technology presented.

Keywords Nanofluidic integration ·
Electrospray ionisation

1 Introduction

Nanofluidic tip based applications have emerged in the form of nanofluidic fountain pens (Deladi et al. 2004; Moldovan et al. 2006; Saya et al. 2007) and nano-electrospray emitters (Legrand et al. 2007; Arscott and Troadec 2005; Mery et al. 2008). These applications require the delivery of fluid to functional nanofluidic tips, possibly arranged in large arrays. Fluidic connection all the way up to the tip has mostly been achieved by capillary slots or by extending nanochannels from fluid reservoirs. Hug et al. (2006) demonstrated the possibility to couple large micro-sized channels to nanochannels using wet oxidation of channels located at the interfaces between two bonded silicon wafers. In this article a fluidic via technology is presented that allows for coupling of microchannels to nanochannels located anywhere on the wafer surface. Microchannel fluidic networks are created beneath the wafer surface, facilitating the leak-tight chemical-inert delivery of fluid from macro-fluidic connections to nanochannels. The mechanical strength of the microchannels can furthermore be utilised in making long freely suspended probes, with a nanochannel positioned right at the tip. The microchannels deliver fluid at low hydrodynamic resistance and large fluid volume ratios compared to connected nanochannels.

In this article nano-slit electrospray emitters are presented, fabricated by the via technology. Koster and Verpoorte (2007) presented a detailed review on microfluidics coupled to electrospray mass spectrometry (ESI-MS). A clear trend in on-chip integrated electrospray emitters was observed. In electrospray ionisation (ESI), reducing emitter aperture size is actively being pursued (Arscott and Troadec 2005; Mery et al. 2008; Gibson et al. 2009; Sikanen et al. 2010), because of smaller droplets

M. Dijkstra · J. W. Berenschot · M. J. de Boer ·
T. S. J. Lammerink · R. J. Wiegink · M. Elwenspoek ·
N. R. Tas (✉)
Transducers Science and Technology,
MESA+ Institute for Nanotechnology,
University of Twente, 7500 AE, Enschede,
The Netherlands
e-mail: n.r.tas@ewi.utwente.nl

H. J. van der Linden · T. Hankemeier
Division of Analytical Biosciences, LACDR, Leiden University,
Einsteinweg 55, 2333 CC Leiden, The Netherlands

being generated. The enhanced ionisation efficiency obtained is of use to proteomics (Valaskovic et al. 1995) and metabolomics. The via technology presented, provides a method to combine emitters, having nano-slit apertures, with microfluidics in a monolithic electrospray chip.

2 Experimental

2.1 Micro- to nanofluidic via technology

Fabrication of the electrospray chips commences with the creation of microchannels beneath the wafer surface for the on-chip delivery of bulk fluid, applying the surface channel concept (Dijkstra et al. 2007). The microchannels are formed by isotropic dry etching of the silicon wafer through 2- μm wide etch holes in a 500-nm silicon-rich silicon nitride (SiRN) layer. The etch holes are closed by a second 1.3- μm SiRN low-pressure chemical vapour deposition (LPCVD), while the inside surface of the etched profile in the silicon wafer is simultaneously conformally coated. Microfluidic devices fabricated with this concept (e.g., a thermal flow sensor by Dijkstra et al. 2008) can readily be integrated with nanochannels using the via technology presented.

Fluidic vias are created by specifically designed etch holes 1- μm wider, preventing them from closing during the second SiRN deposition. Plugs are inserted in the open vias by 1- μm poly-Si LPCVD deposition and patterning (see - Fig. 1a), where the deposition rate inside the microchannels was found to decrease with distance from the via.

The sealed microchannels leave a nearly planar wafer surface on which nanochannels (4 $\mu\text{m} \times 200 \text{ nm}$) are connected to the poly-Si plugs (see Fig. 1b), applying a 200-nm sacrificial poly-Si layer and a 200-nm SiRN capping layer. Nano-lithographical methods (e.g. Luttge et al.

2007) can be applied to integrate nanochannels with even smaller dimensions.

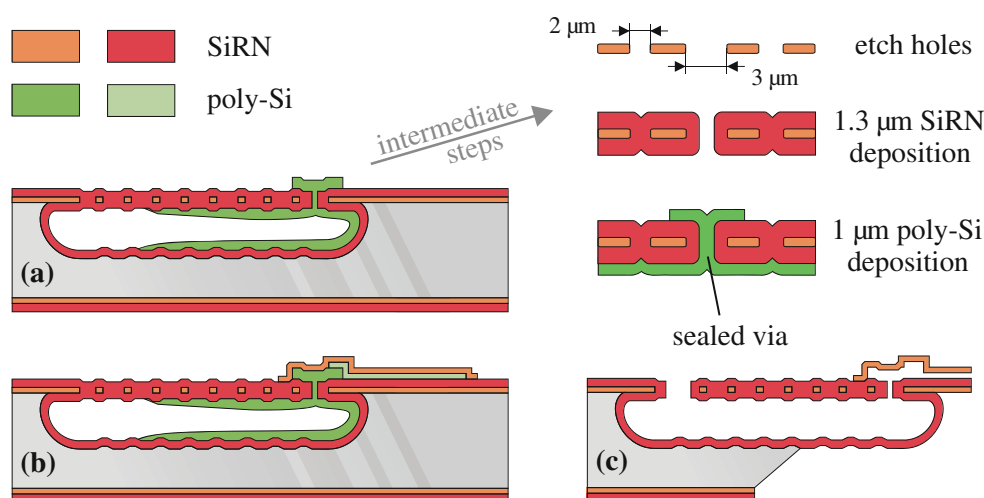
Electrospray chips were released using KOH 25wt% at 75°C (Berenschot et al. 2002), where the sacrificial poly-Si inside the nanochannels is etched after inlets and outlets have been created (see Fig. 1c). Only in cases where etching occurs from a nanochannel into a sealed microchannel without an outlet, was it observed that via connections often break. This is caused by a sudden increase in H_2 gas produced due to a large surface array of poly-Si being exposed inside the microchannel. The process wafers where RCA-2 cleaned after KOH etching and left in de-ionised water for several days.

Figure 2 shows a fabricated electrospray probe with a 60- μm long nanochannel, where the inset in Fig. 2b shows a focused ion-beam (FIB) cut through the fluidic via connection between micro- and nanochannel.

2.2 Filling experiments

Filling experiments were done using $\text{H}_2\text{O}:\text{MeOH}$ (50:50v%) solution, where the surface tension of the liquid drives the capillary filling (Tas et al. 2004). A contact angle of 15° was measured for the $\text{H}_2\text{O}:\text{MeOH}$ (50:50v%) solution on the cleaned SiRN surface of one of the process wafers. Capillary filling of the microchannel on the electrospray tip (Fig. 2) was found to be restricted by the large volume of air in the microchannel, which needs to be pushed out through the nanochannel. This was confirmed by preparing several nanochannel lengths from the initial 60- μm long nanochannel (Fig. 2) by FIB cutting, where the filling speed was found to be constant in time during restricted capillary filling and inversely proportional to the nanochannel length. Subsequent refilling of previously filled electrospray chips resulted in instant wetting of the via and nanochannel with the formation of bubbles along the

Fig. 1 Process schematic for the fabrication of via connections between surface microchannels (Dijkstra et al. 2007) and sacrificial nanochannels, with **a** fabrication of a via through the surface microchannel (see intermediate steps), **b** fabrication of the nanochannel and **c** bottom- and topside etching of SiRN layers, where simultaneously openings are etched in the micro- and nanochannel, followed by KOH release of the electrospray chip



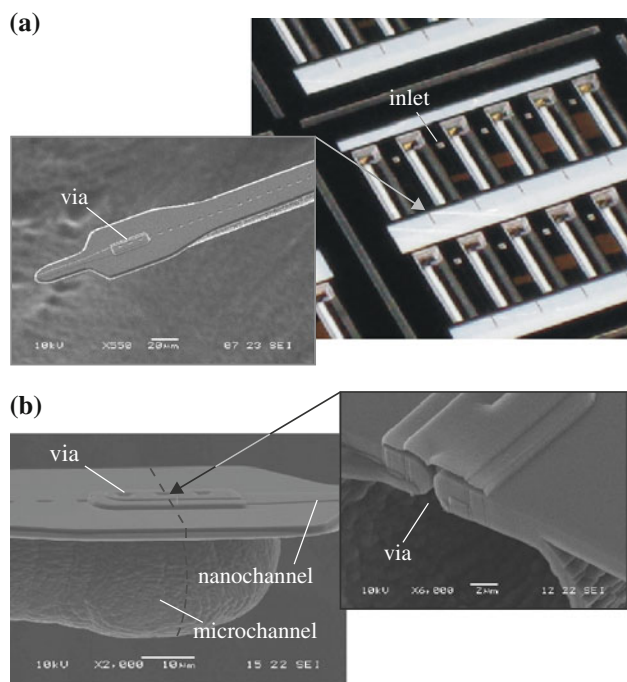


Fig. 2 Electro spray chips, where **a** the *inset* shows a nano-slit electro spray emitter suspended on a microchannel probe and **b** micrographs of the via connection between nanochannel and microchannel, where the *inset* shows a FIB cut through the fluidic via

microchannel, likely due to a long-term remaining saturated atmosphere in the microchannels.

An additional fluidic chip was fabricated to study filling mechanisms, containing freely suspended nanochannels, connected to separate microchannels on either side for the transport of fluid (see Fig. 3). The filling of the chip was studied by applying $\text{H}_2\text{O}:\text{MeOH}$ (50:50v%) solution at the inlets of the microchannels connected to the lower part of the nanochannels in Figs. 3 and 4, while the microchannels on the upper part were not filled.

Figure 4 shows subsequent snapshots taken, during filling of the chip, where after 1.8 s the fluid reaches the via connections, where the air in the microchannels is pushed out through the microchannel outlets. The fluid then enters through the fluidic vias into the nanochannels. The nanochannels filled rapidly around 4.4 s, with a visible corner flow (Dong and Chatzis 1995) preceding the bulk fluid. After 6.2 s air bubbles are trapped by fluid appearing from the opposite end and only slowly dissolve until the nanochannels are completely filled at 42 s. The liquid appearing on opposite ends is caused by additional transport mechanisms, possibly vapour diffusion, film flow and corner flow (Eijkel et al. 2005). The pinning of the fluid contact line (Ondařuhu and Piednoir 2005) at the fluidic via connections on the opposite ends of the nanochannels prevents further capillary filling of the connected microchannels.

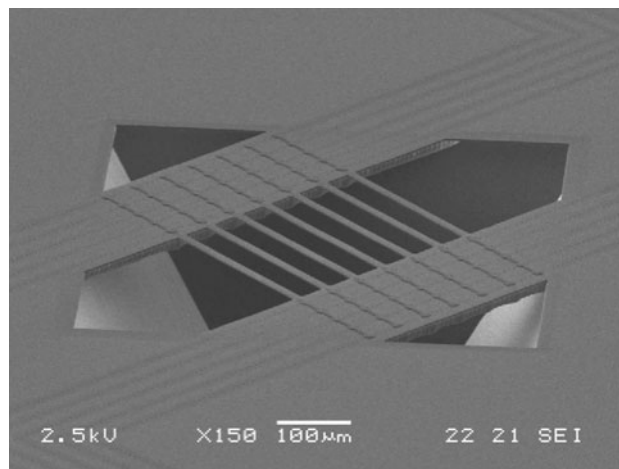


Fig. 3 Micrograph of freely suspended nanochannels connected to microchannels for the on-chip transport of fluid

2.3 Nano-slit electro spray emitters

A redesign of the nanochannel electro spray emitter was made based on experimental filling results, taking the effect of additional transport mechanisms (Dong and Chatzis 1995; Eijkel et al. 2005) and gas-flow restriction on the filling behaviour into consideration. Electro spray chips were batch fabricated containing microchannel probes with integrated nano-slit emitters, where the nanochannel length was designed to be $3\text{ }\mu\text{m}$ (see Fig. 5), facilitating the fast filling of the microchannel. With the redesign, electro spraying can be performed from multiple emitters, while the air inside the microchannel can easily escape during capillary filling of the fluidic chip.

Additional designs were made, where the nano-slit emitters are integrated on a continuous microchannel, such that a crossflow can pass the emitters (see Fig. 6). This eliminates problems with air bubbles remaining in the microchannel and even electro spraying from a continuous flow can be achieved.

2.4 Electro spray ionisation setup

Both the nanochannel electro spray chip after FIB cutting (similar to inset in Fig. 2a) and the nano-slit emitter chip (Fig. 5) were used for electro spraying. A Keithley 237 high-voltage source-measurement unit (SMU) was used to apply an electric field (see Fig. 7). Triax-cable connections with active guarding were used for high-spray current resolution. The electro spray chip was filled with spraying solution and a probe needle was inserted in the inlet. The counter electrode was isolated from the rest of the setup using a Teflon rod, with at least several $\text{T}\Omega$ resistance. The counter electrode distance to the emitter was determined

Fig. 4 Several snapshots taken during the filling with $\text{H}_2\text{O}:\text{MeOH}$ (50:50v%) solution of freely suspended nanochannels. Each frame has been enhanced with the same image filters

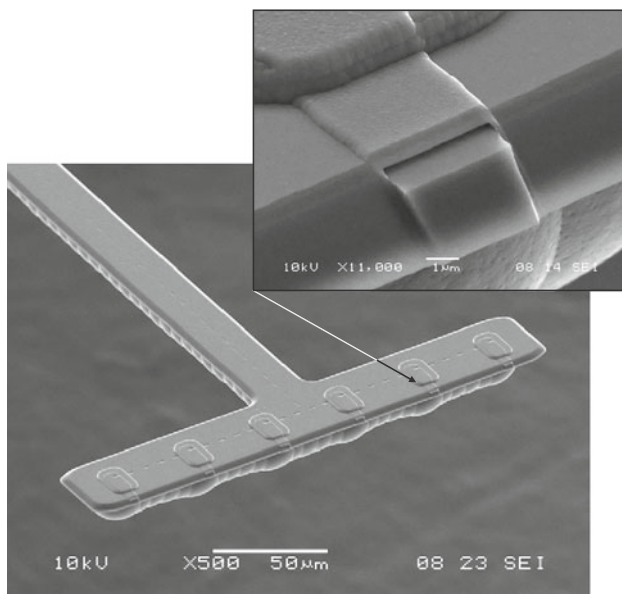
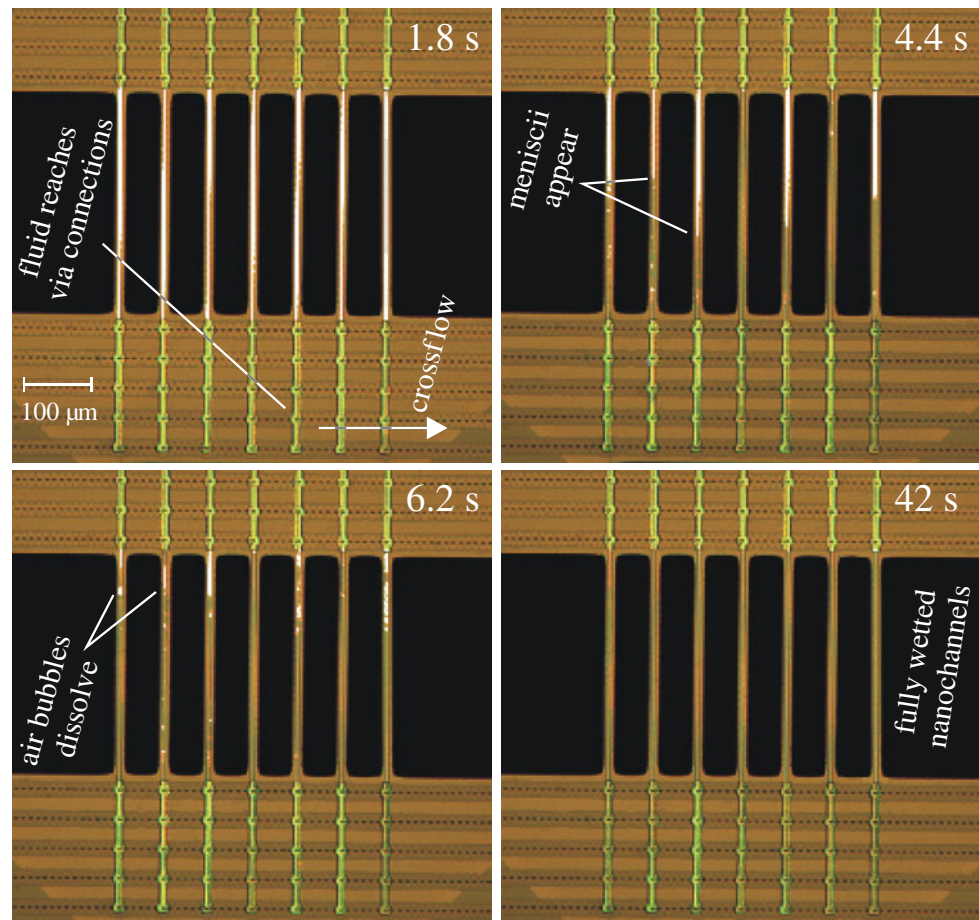


Fig. 5 Micrographs of nano-slit electrospay emitters on a micro-channel probe. The *inset* shows a nano-slit emitter, with $4\ \mu\text{m} \times 200\ \text{nm}$ aperture size

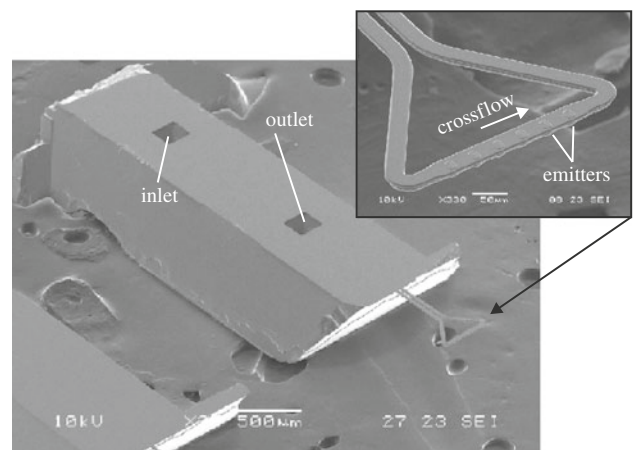


Fig. 6 Micrographs of nano-slit electrospay emitters, where a crossflow can pass the nano-slit emitters from an on-chip inlet to an outlet

using an adjustable micrometre, with roughly $2\text{-}\mu\text{m}$ resolution. With the setup, pA resolution was obtained up to 1.1-kV counter electrode voltage applied. Without

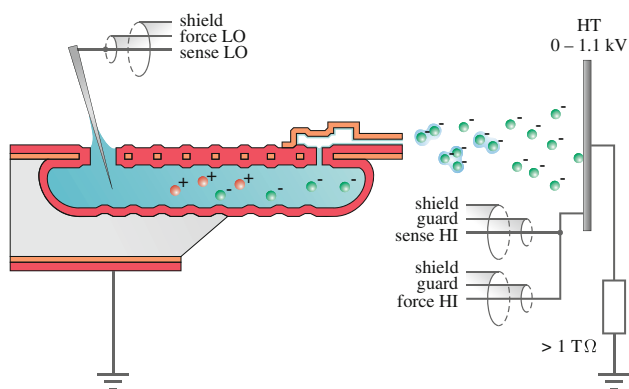


Fig. 7 Electro spraying from nano-slit emitter, with pA resolution, using the Keithley 237 high-voltage SMU and triax-cable connections. The counter electrode was isolated with $>1\text{ T}\Omega$ resistance in reference to the remainder of the setup

spraying, IV-curves show hysteresis due to capacitive effects in cabling and the solution inside the microchannel. Therefore, an 8-s delay was used between applying counter electrode voltage and acquisition of the spray current.

3 Results and discussion

Initially electro spray IV-curves were obtained on a fully wetted nanochannel emitter (similar to Fig. 2a) reduced in length with FIB to $15\text{ }\mu\text{m}$, using $\text{H}_2\text{O}:\text{MeOH}$ (50:50v%) solution, without back pressure applied. Repeatable IV-curves in the nA range were obtained at various distances of the emitter to the cathode (see Fig. 8). The spray current is generally very stable (small standard deviation) near the onset of spraying, taking 6 min to acquire a single IV-curve. The individual IV-curves are monotonically increasing near the onset of spraying and are less stable at higher electro spray voltages. The ion concentration at the emitters remains nearly constant due to the low hydrodynamic resistance of the microchannel for the advection of ion species. The onset voltage is, therefore, determined by the emitter geometry, stable ion concentration and applied electric field. The applied potential causes polarisation of both the liquid and the dielectric SiRN of the freely suspended microchannel, lowering the effective electric field strength between nano-slit emitters and counter electrode. This explains a higher onset voltage compared to Arscott and Troadec (2005).

Subsequently several nano-slit emitter chips (Fig. 5) were filled with $\text{H}_2\text{O}:\text{MeOH}$ (50:50v%) solution for spraying. However, during capillary filling the solution did not fully wet the nano-slit emitters. The microchannels always filled completely, but the fluid contact line did not cross the fluidic vias. The fluidic chip with freely

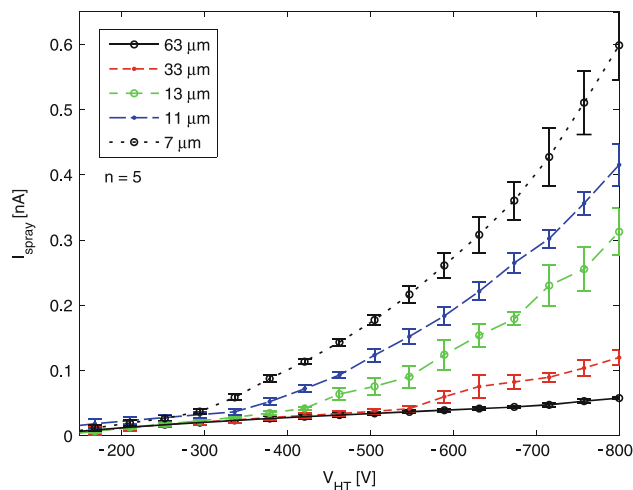


Fig. 8 Electro spray IV-curves measured on a fully wetted FIB cut $15\text{-}\mu\text{m}$ nanochannel emitter (similar to Fig. 2a) at various distances to the cathode, using $\text{H}_2\text{O}:\text{MeOH}$ (50:50v%) solution ($4.6\text{ }\mu\text{S}/\text{cm}$)

suspended nanochannels (similar to Fig. 3), also fabricated on the same wafer, did, however, fill with the same $\text{H}_2\text{O}:\text{MeOH}$ (50:50v%) solution. It is likely that the fluid contact line is pinned on the fluidic vias, which can be overcome when a saturated atmosphere develops inside the nanochannel. This can explain the unsuccessful filling of the $3\text{-}\mu\text{m}$ short nano-slit emitters, which cannot develop a saturated atmosphere due to a high evaporation rate. Remarkably, using a high-conductive $\text{H}_2\text{O}:\text{MeOH}$ (50:50v%) + CH_3COOH (1v%) solution electro spray IV-curves could be obtained from unfilled nano-slit emitters (Fig. 5). The exact spraying mechanism is currently not understood. It is possible that nano-sized droplets are directly sprayed from the nano-slit emitters (Juraschek et al. 1999).

IV-curves, at various distances to the anode, were obtained (see Fig. 9). The emitters were aligned with the counter electrode by manual adjustments and microscope observations close to the counter electrode. During the last IV-curve measurement point at $8\text{-}\mu\text{m}$ distance, it was observed that the nano-slit emitter closest to the anode, due to a small angular misalignment, became fully wetted. The strong electric field apparently pulled the fluid contact line through the fluidic via. The spray current instantly became 20 nA , which was set as current limit. The electro spray chip was taken for SEM inspection directly after the electro spray measurement. Figure 10 shows traces left by the fluid outside of the wetted nano-slit emitter, where the sample was SEM coated before inspection. The SEM coating process made the meniscus visible by deposition of coating material. The other emitters were no different from emitters inspected just after fabrication, confirming that the IV-curves in Fig. 9 were obtained on unfilled emitters.

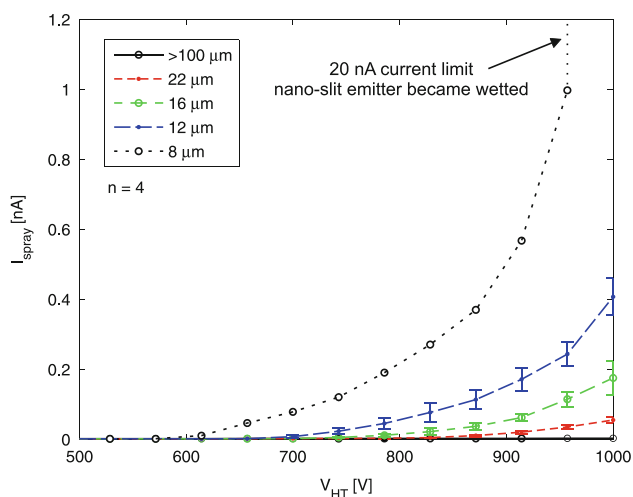


Fig. 9 Electro spray IV-curves measured on unfilled nano-slit emitters (Fig. 5) at various distances to the anode, using $\text{H}_2\text{O}:\text{MeOH}$ (50:50v%) + CH_3COOH (1v%) solution (120 $\mu\text{S}/\text{cm}$)

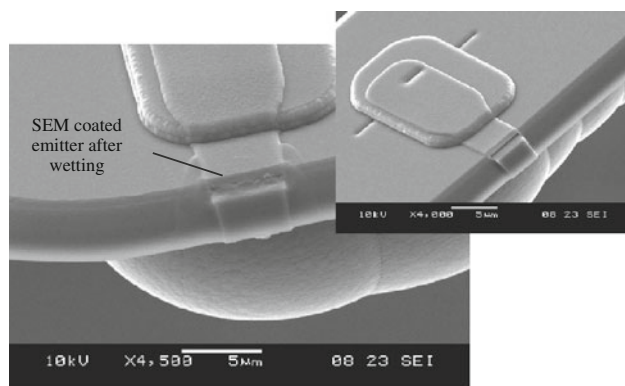


Fig. 10 Micrographs of the SEM coated nano-slit emitter, wetted during electro spraying at 8- μm anode distance applying 1 kV, compared to unfilled emitter on the same sample observed after spraying

4 Conclusions

A novel micro- to nanofluidic via technology has been presented. It was demonstrated that bulk fluid can be transported from macro-fluidic connections to on-chip nanochannels. The technology has shown potential in applications where on-chip freely suspended nanochannels are required. The capillary filling of fluidic chips was studied and it was concluded that additional transport mechanisms, gas-flow restriction and pinning of fluid contact lines have to be considered when designing coupled micro- to nanofluidic devices. Better understanding of these transport mechanisms during filling is required for the via technology to be applicable to other fluidic designs. Proper capillary filling of microchannels can, however, be achieved by crossflow filling of connected nanochannels.

Repeatable electro spray IV-curves were obtained on nano-slit emitters, despite the fact that the emitters did not fully wet. This provides for an interesting spraying mode, which requires further investigation. Especially, the size distribution of possibly emitted nano-droplets, compared to fully wetted emitters, is of interest.

The prospect of the nano-slit electro spray chip presented is to increase emitter density, while reducing aperture size. Nano-droplet emission at higher densities can then be achieved. Furthermore, the microchannel can be utilised to include a high-pressure liquid chromatography (HPLC) column, where HPLC packing material can be packed up to the nano-slit emitters (Fig. 6). Additionally, capillary electrophoresis (CE) and microfluidic devices can be integrated on-chip.

Acknowledgments The authors would like to acknowledge J.G.M. Sanderink for his assistance with FIB operation.

Open Access This article is distributed under the terms of the Creative Commons Attribution License which permits any use, distribution, and reproduction in any medium, provided the original author(s) and the source are credited.

References

- Arscott S, Troadec D (2005) Electro spraying from nanofluidic capillary slot. *Appl Phys Lett* 87(13):134101
- Berenschot JW, Tas NR, Lammerink TSJ, Elwenspoek M, van den Berg A (2002) Advanced sacrificial poly-Si technology for fluidic systems. *J Micromech Microeng* 12(5):621–624
- Deladi S, Tas NR, Berenschot JW, Krijnen GJM, de Boer MJ, de Boer JH, Peter M, Elwenspoek MC (2004) Micromachined fountain pen for atomic force microscope-based nanopatterning. *Appl Phys Lett* 85(22):5361–5363
- Dijkstra M, de Boer MJ, Berenschot JW, Lammerink TSJ, Wiegink RJ, Elwenspoek M (2007) A versatile surface channel concept for microfluidic applications. *J Micromech Microeng* 17(10):1971–1977
- Dijkstra M, de Boer MJ, Berenschot JW, Lammerink TSJ, Wiegink RJ, Elwenspoek M (2008) Miniaturized thermal flow sensor with planar integrated sensor structures on semicircular surface channels. *Sens Actuator A Phys* 143(1):1–6
- Dong M, Chatzis I (1995) The imbibition and flow of a wetting liquid along the corners of a square capillary tube. *J Colloid Interf Sci* 172(2):278–288
- Eijkel JCT, Dan B, Reemeijer HW, Hermes DC, Bomer JG, van den Berg A (2005) Strong accelerated and humidity-independent drying of nanochannels induced by sharp corners. *Phys Rev Lett* 95(256107):1–4
- Gibson GTT, Mugo SM, Oleschuk RD (2009) Nanoelectrospray emitters: trends and perspective. *Mass Spectrom Rev* 28(6):918–936
- Hug TS, de Rooij NF, Staufer U (2006) Fabrication and electroosmotic flow measurements in micro- and nanofluidic channels. *Microfluid Nanofluid* 2(2):117–124
- Juraschek R, Dülcks T, Karas M (1999) Nanoelectrospray—more than just a minimized-flow electro spray ionization source. *J Am Soc Mass Spectr* 10(4):300–308

- Koster S, Verpoorte E (2007) A decade of microfluidic analysis coupled with electrospray mass spectrometry: an overview. *Lab Chip* 7(11):1394–1412
- Legrand B, Ashcroft AE, Buchaillot L, Arscott S (2007) SOI-based nanoelectrospray emitter tips for mass spectrometry. *J Micromech Microeng* 17:509–514
- Luttge R, van Wolferen HAGM, Abelman L (2007) Laser interferometric nanolithography using a new positive chemical amplified resist. *J Vac Sci Technol B* 25(6):2476–2480
- Mery E, Ricoul F, Sarrut N, Constantin O, Delapierre G, Garin J, Vinet F (2008) A silicon microfluidic chip integrating an ordered micropillar array separation column and nano-electrospray emitter for LC/MS analysis of peptides. *Sens Actuator B Chem* 134(2):438–446
- Moldovan N, Kim K-H, Espinosa HD (2006) A multi-ink linear array of nanofountain probes. *J Micromech Microeng* 16(10):1935–1942
- Ondarçuhu T, Piednoir A (2005) Pinning of a contact line on nanometric steps during the dewetting of a terraced substrate. *Nano Lett* 5(9):1744–1750
- Saya D, Leïchl   T, Pourciel JB, Bergaud C, Nicu L (2007) Collective fabrication of an in-plane silicon nanotip for parallel femtoliter droplet deposition. *J Micromech Microeng* 17(1):N1–N5
- Sikanen T, Franssila S, Kauppila TJ, Kostainen R, Kotiaho T, Ketola RA (2010) Microchip technology in mass spectrometry. *Mass Spectrom Rev* 29(3):351–391
- Tas NR, Haneveld J, Jansen HV, Elwenspoek M, van den Berg A (2004) Capillary filling speed of water in nanochannels. *Appl Phys Lett* 85(15):3274
- Valaskovic GA, Kelleher NL, Little DP, Aaserud DJ, McLafferty FW (1995) Attomole-sensitivity electrospray source for large-molecule mass spectrometry. *Anal Chem* 67(20):3802–3805